Session V - Additive Manufacturing

S5 - 1

DIFFRACTION AND SINGLE-CRYSTAL ELASTIC CONSTANTS OF LASER POWDER BED FUSED INCONEL 718

J. Schröder[1], A. Evans[1], A. Heldmann[2], M. Hofmann[2], E. Polatidis[3], J. Čapek[3], I. Serrano-Munoz[1], W. Petry[2], G. Bruno[1, 4]

[1]Bundesanstalt für Materialforschung und -prüfung, Unter den Eichen 87, 12205 Berlin, Gemany
[2]Heinz Maier-Leibnitz Zentrum, Technische Universität München, Lichtenbergstraße 1, 85748 Garching b. München, Germany
[3]Laboratory for Neutron Scattering and Imaging, Paul Scherrer Institut, Forschungsstrasse 111, 5232 Villigen, Switzerland
[4]Universität Potsdam, Institut für Physik und Astronomie, Karl-Liebknecht-Str. 24-25, 14476 Potsdam, Germany
Jakob.Schroeder@bam.de

Laser powder bed fusion (PBF-LB/M) of metallic alloys is a layer-wise additive manufacturing process that provides significant scope for more efficient designs of components, benefiting performance and weight, leading to efficiency improvements for various sectors of industry. However, to benefit from these design freedoms, knowledge of the high produced induced residual stress and mechanical property anisotropy associated with the unique microstructures is critical. X-ray and neutron diffraction are considered the benchmark for non-destructive characterization of surface and bulk internal residual stress. The latter, characterized by the high penetration power in most engineering alloys, allows for the use of a diffraction angle close to 90° enabling a near cubic sampling volume to be specified. However, the complex microstructures of columnar growth with inherent crystallographic texture typically produced during PBF-LB/M of metallics present significant challenges to the assumptions typically required for time efficient determination of residual stress. These challenges include the selection of an appropriate set of diffraction elastic constants and a representative lattice plane suitable for residual stress analysis. In this contribution, the selection of a suitable lattice plane family for residual stress analysis is explored. Furthermore, the determination of an appropriate set of diffraction and single-crystal elastic constants depending on the underlying microstructure is addressed.

In-situ loading experiments have been performed at the Swiss Spallation Neutron Source [1] with the main scope to study the deformation behaviour of laser powder bed fused Inconel 718. Cylindrical tensile bars have been subjected to an increasing mechanical load (Fig. 1). At pre-defined steps, neutron diffraction data has been collected. After reaching the yield limit, unloads have been performed to study the accumulation of intergranular strain among various lattice plane families (Fig. 2).

On the one hand, it was revealed that the presence of texture controls the accumulation of residual microstrain. However, overall, the 311 reflection remains the best compromise for performing residual stress analysis in laser powder bed fused Inconel 718. On the other hand, it was shown that the lattice plane specific elastic moduli do not show large variations for specimens possessing different crystallographic textures.

To determine the diffraction and single-crystal elastic constants of laser powder bed fused Inconel 718, an in-situ loading experiment has been performed at the High-energy materials science beamline at the Deutsches-Elektronen Synchrotron DESY (Fig. 3). In the general case, the diffraction elastic constants are expressed by the so-called stress factors. When a uniaxial stress is applied, their deter-

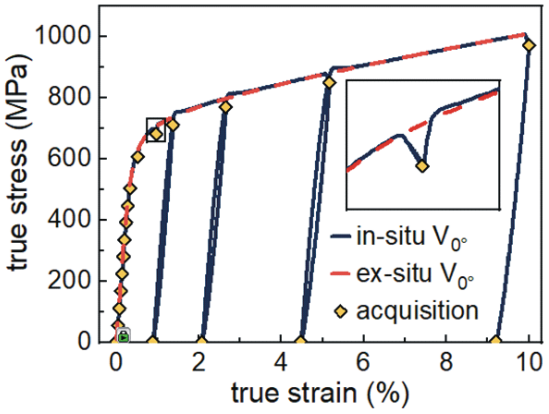

Figure 1. True stress-strain curve during in-situ loading [1].

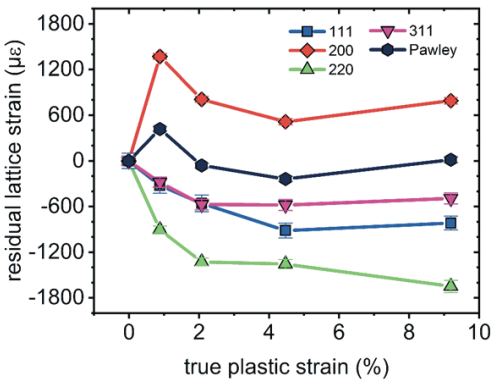

Figure 2. Residual strain accumulation of various lattice planes [1].

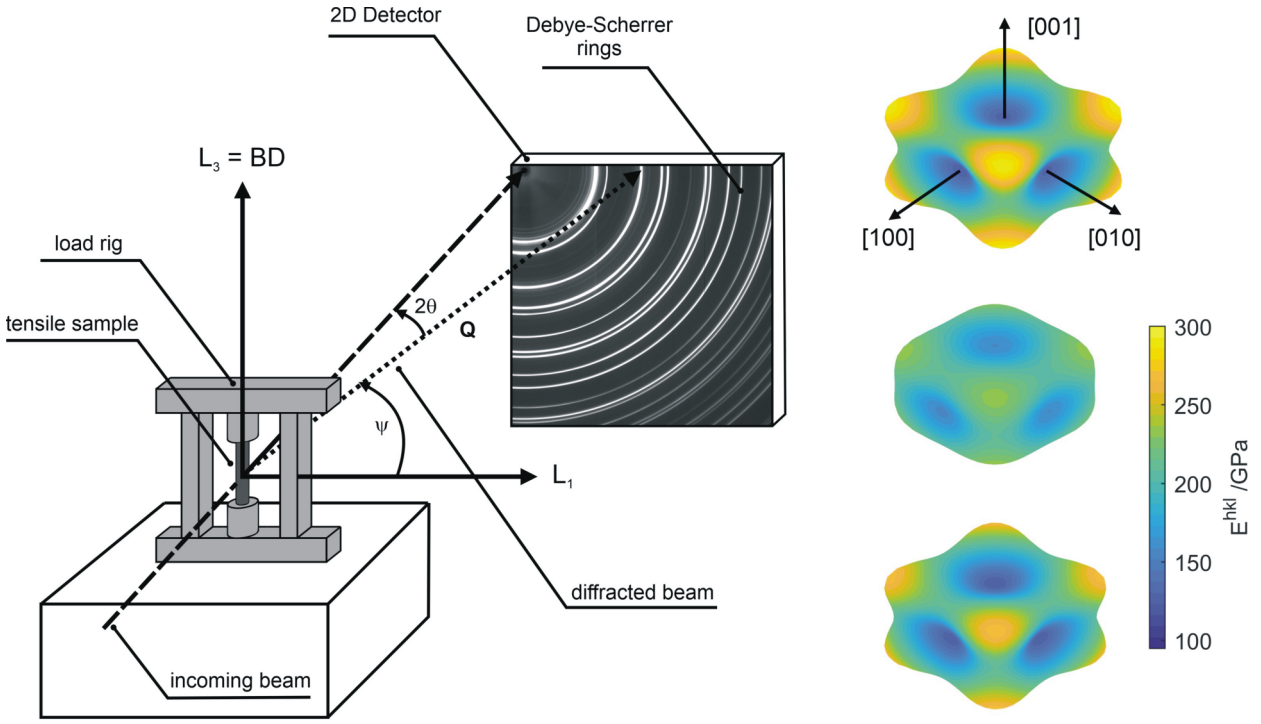

Figure 3. Determination of diffraction and single-crystal elastic constants [2].

mination is a simple application of Hooke's law through a linear regression of lattice strain of reflection hkl as a function of the applied stress eq. (1) [3, 4]. Even though the specimen possessed crystallographic texture it was found that the definition of quasi-isotropic diffraction elastic constants remains acceptable (i.e., the behaviour follows a linear trend over $\cos^2\psi$). This is particularly true for lattice plane families possessing a high multiplicity (i.e., hkk reflections).

$$\overline{\varepsilon_{33}^{L}}(\varphi,\Psi,hkl)=\frac{d(\varphi,\Psi,hkl)-d_0(\varphi,\Psi,hkl)}{d_0(\varphi,\Psi,hkl)}= \\ =\frac{\partial\overline{\varepsilon_{33}^{L}}(\varphi,\Psi,hkl)}{\partial\overline{\sigma}_{ij}}=F_{33ij}(\varphi,\Psi,hkl)\overline{\sigma}_{ij} \quad (1)$$

By an inversion of the calculations of micromechanical models, a set of single-crystal elastic constants can be refined using the experimental diffraction elastic constants (Fig. 3). Each refined set of single-crystal elastic constants is representative of the model's assumptions.

1. J. Schröder, A. Evans, E. Polatidis, J. Čapek, G. Mohr, I. Serrano-Munoz, G. Bruno, J. Mater. Sci, **57**, (2022), 15036-15058.
2. J. Schröder, A. Heldmann, M. Hofmann, A. Evans, W. Petry, G. Bruno, Mater. Lett.
3. Dölle, H. & Hauk, V. (1978). Z. Metallkd. 69, 410–417.
4. Dölle, H. & Hauk, V. (1979). Z. Metallkd. 70, 682–685.

S5 - 2

OPTIMIZING RESIDUAL STRESSES IN ADDITIVELY MANUFACTURED HIGH-PERFORMANCE MATERIALS THROUGH ULTRASONIC-ASSISTED MILLING

J. Witte, L. Engelking, D. Schroepfer, T. Kannengiesser

Bundesanstalt für Materialforschung und -prüfung (BAM), Unter den Eichen 87, 12205 Berlin, Germany
Julien.Witte@bam.de

The integration of modern high-performance materials in combination with additive manufacturing (AM) has revolutionized the approach to lightweight construction across diverse applications. This study explores the synergy between these materials and additive manufacturing (AM), focusing on their unique properties to engineer resource-efficient structures. Despite these advancements, machining these difficult-to-cut materials such as iron-aluminide or nickel alloys (e.g. alloy 36) for safety-relevant components remains challenging due to increased tool wear and compromised surface integrity. This research focuses on overcoming these challenges through the application of ultrasonic-assisted milling (USAM), a hybrid machining process exhibiting significant potential. By incorporating ultrasonic oscillations along the milling tool axis, USAM minimizes tool and component surface loads, enhancing tool life and generating defect-free, homogeneous surfaces with reduced roughness parameters. This investigation focuses on the influence of USAM on residual stresses, crucial for component performance under load. In contrast to conventional milling (CM) generating undesirable tensile residual stresses, USAM induces advantageous compressive residual stresses which have a positive effect in terms of crack propagation control, corrosion resistance and fatigue life [1-3]. In this investigation, machining experiments were carried out on conventionally manufactured die-cast samples made of iron-aluminide and wire arc additive manufactured components made of alloy 36 and a modification with 0.4 wt.-% Zr. In addition to the cutting speed v_c and the feed rate f_z, the amplitude of the USAM process A_{US} is varied to identify optimal parameters for achieving maximum surface-near compressive residual stresses.

Figure 1 shows for the modification of alloy 36 with 0.4 wt.-% Zr the maximal principal residual stresses σ_{max} versus cutting speed and feed rate for a) conventional milling and b) ultrasonic-assisted milling. The CM process mainly causes the formation of tensile residual stresses and the USAM process induces compressive residual stresses. The feed rate has no significant influence on the residual stresses for both milling processes. An increase in the cutting speed causes an increase in the residual stresses for the CM process and a decrease for the USAM process. The cause of this interaction is the number of oscillations per cutting engagement, which is determined by the ultrasonic frequency and cutting speed.

The amplitude of the ultrasonic oscillation A_{US} shows significant impact on residual stresses in Figure 2. While the unmachined sandblasted surface showed compressive residual stress, the conventional milling at 0% ultrasonic power P_{US} resulted in tensile residual stresses on the component surface. Ultrasonic-assisted milling, on the other hand, shows residual compressive stresses regardless of the power selected, with a maximum at 40%. Furthermore, electrochemical ablation was employed to investigate the depth profile of these residual stresses in Figure 3. The findings indicated that ultrasonic-assisted milling induced compressive stresses up to a depth of 80 µm from the surface, providing more precise insights into their distribution and potential effects.

This research not only contributes to the evolving environment of innovative manufacturing technologies, but also places particular focus on the central role of residual stresses in the performance and reliability of safety-relevant AM components in real-life applications.

1. E. Salvati, H. Zhang, K.S. Fong, X. Song, A.M. Korsunsky, Separating plasticity-induced closure and resid-

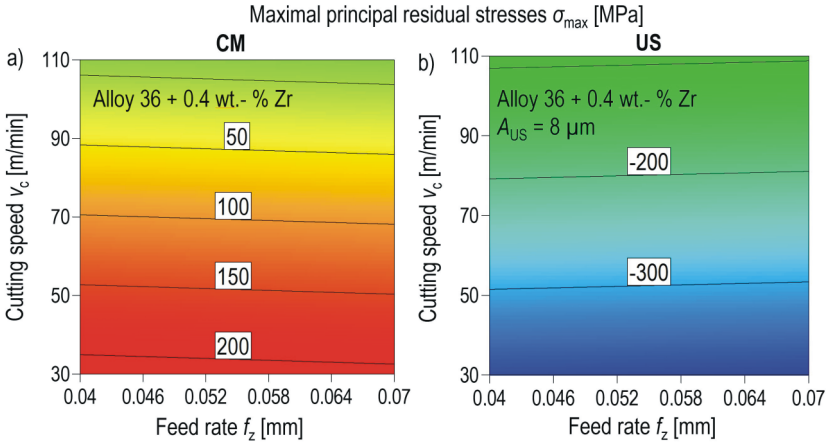

Figure 1. Maximal principal residual stresses σ_{max} versus cutting speed v_c and feed rate f_z for a) conventional milling and b) ultrasonic-assisted milling.

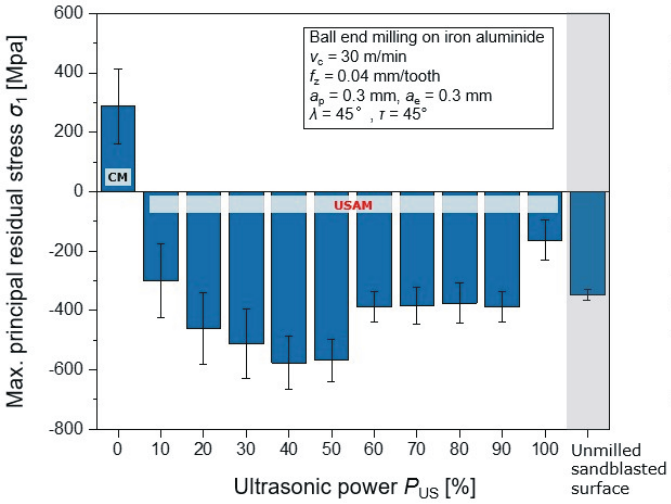

Figure 2. Maximal principal residual stresses σ_{max} under variation of the ultrasonic power P_{US}.

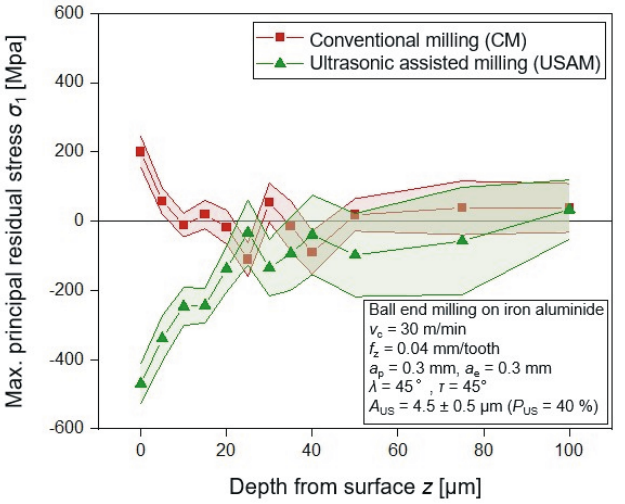

Figure 3. Comparison of the maximal principal residual stresses σ_{max} in the depth from surface z between conventional and ultrasonic assisted milling.

ual stress contributions to fatigue crack retardation following an overload, Journal of the Mechanics and Physics of Solids 98 (2017) 222-235.

2. N. Masmiati, A.A.D. Sarhan, M.A.N. Hassan, M. Hamdi, Optimization of cutting conditions for minimum residual stress, cutting force and surface roughness in end milling of S50C medium carbon steel, Measurement 86 (2016) 253-265.

3. E. Mirkoohi, P. Bocchini, S.Y. Liang, Inverse analysis of residual stress in orthogonal cutting, Journal of Manufacturing Processes 38 (2019) 462-471.

S5 - 3

INFLUENCE OF COMPONENT GEOMETRY ON RESIDUAL STRESS IN ADDITIVELY MANUFACTURED ALUMINIUM STRUCTURES

M.-A. Nielsen[1], S. Bodner[2], E. Maawad[1], F. Resch[3], J. Keckes[2], G. Abreu Faria[1], P. Staron[1], M. Müller[1]

[1]Institute of Materials Physics, Helmholtz-Zentrum Hereon, Germany
[2]Erich Schmid Institute, Montanuniversität Leoben, Austria
[3]Resch GmbH, Glojach, Austria
marc-andre.nielsen@hereon.de

Additive manufacturing (AM) opens up new ways to produce parts with high geometric complexity, e.g. involving internal structures, which led to an increased interest of science and industry in the recent years [1]. The mechanical behavior and load-bearing capacity of additively manufactured components, however, are still not completely understood and subject of intensive research efforts [2]. In particular, residual stresses (RS) play an important role for the strength and fatigue properties. Therefore, RS distributions were investigated in various parts, fabricated from aluminium alloy powder (AlSi10Mg) using the Laser Powder Bed Fusion (LPBF) technique.

Residual stress fields were determined using high-energy X-ray diffraction using Hereon beamlines at Petra III at Deutsches Elektronen Synchrotron (DESY). High photon energies were used to allow penetration of thicker structures. Angle-dispersive diffraction was used in transmission geometry and energy-dispersive techniques were used to obtain three-dimensional spatial resolution.

Different structures with increasing complexity were produced to study the influence of geometry on the RS distribution. Thin walls are the simplest structures, showing an influence of edge geometry. The RS fields get more complex with increasing geometrical complexity, e.g. for tubes or honeycomb structures. The principal stress directions were observed to rotate in a honeycomb structure. Typical stress distributions will be shown and discussed in context with the specific microstructure of the AM parts.

1. Yang, L., et al., Additive manufacturing of metals: the technology, materials, design and production. 2017: Springer.

2. Campbell, I., et al., Wohlers report 2018: 3D printing and additive manufacturing state of the industry: annual worldwide progress report. 2018: Wohlers Associates.

S5 - 4

MICROSTRUCTURE AND STRESS EVOLUTION DURING LASER DIRECTED ENERGY DEPOSITION OF TOOL STEEL BY *IN-SITU* SYNCHROTRON X-RAY DIFFRACTION

Antonio Carlos de F. Silveira[1], Jeremy Epp[1,2]

[1]Leibniz-Institute fuer Werkstofforientierte Technologien-IWT, Germany
[2]MAPEX Center for Materials and Processes, University of Bremen, Bibliothekstr. 1, 28359, Bremen, Germany
epp@iwt-bremen.de

Laser-directed energy deposition (L-DED) is a process that enables the manufacturing of complex metallic components by depositing multiple layers through the melting of a powder or wire by a laser. The material is melted and cooled down during the deposition with very high heating and cooling rates (10^2 ~10^4 °K.s^{-1}) [1]. Therefore, the generation of stresses is unavoidable and, if excessively high, can create cracks in the part, critically affecting the component performance. In the case of tool steel, the stress state is further affected by the martensitic transformation. Besides the aspects of a single deposition, previous work showed that the multiple layer deposition generates cyclic thermal cycles, further modifying the already deposited material [2,3]. During this step, also called Intrinsic heat treatment (IHT), several metallurgical modifications can occur, for example, dislocation annihilation, martensite tempering, carbide precipitation, etc. [4]. All these changes further influence the stresses in the material and will be responsible for the final residual stress state in the finished part. Hence, understanding how these complex overlapped effects influence the stresses during the L-DED becomes crucial in developing AM processes. For this end, in-situ, high energy synchrotron X-ray diffraction (HEXRD) was done during L-DED manufacturing of thin walls made of tool steel X40CrMoV5-1 (H13). To evaluate the stresses, an approach based on the distortion of the diffracted rings was used, assuming a plane strain state, and considerations were made regarding the elastic constants and the reference d-spacing over a wide temperature range. Additionally, phase transformations as well as the evolution of dislocation density in both austenite and martensite was estimated during the process and related to the microstructural evolution. The results show that stresses in austenite are tensile after solidification and during further cooling until the martensitic transformation takes place, shifting the stresses to compression while introducing lattice defects in the remaining austenite phase. Over the cycles, it could be shown that the stresses vary between tensile and compressive state along the height of the wall, leading to the remaining residual stress state after final cooling.

1. Svetlizky, D.; Das, M.; Zheng, B.; Vyatskikh, A.L.; Bose, S.; Bandyopadhyay, A.; Schoenung, J.M.; Lavernia, E.J.; Eliaz, N., *Mater. Today* 2021, **49**, 271–295. https://doi.org/10.1016/j.mattod.2021.03.020.
2. Silveira, A.C. de F.; Fechte-Heinen, R.; Epp, J., *Addit. Manuf.* 2023, **63**, 103408. https://doi.org/10.1016/j.addma.2023.103408.
3. Epp, J.; Dong, J.; Meyer, H.; Bohlen, A., *Scr. Mater.* 2020, **177**, 27–31. https://doi.org/10.1016/j.scriptamat.2019.09.021.
4. Narvan, M.; Ghasemi, A.; Fereiduni, E.; Kendrish, S.; Elbestawi, *Mater. Des*. 2021, **204**, 109659. https://doi.org/10.1016/j.matdes.2021.109659.

S5 - 5

DIFFRACTION BASED RESIDUAL STRESS ANALYSIS FOR LASER POWDER BED FUSION ALLOYS

A. Evans, I. Serrano-Munoz, J. Schröder, T. Mishurova, I. Roveda, M. Sprengel, T. Fritsch, A. Ulbricht, A. Kromm and G. Bruno

Bundesanstalt für Materialforschung und -prüfung (BAM), Unter den Eichen 87, 12205 Berlin, Germany
alexander.evans@bam.de

Laser Powder Bed Fusion (PBF-LB/M) is a layer wise metal additive manufacturing (AM) technology, which enables significant advancements of component design, leading to potential efficiency and performance improvements. However, the thermal cycles inherent to the process comprising large localized thermal gradients and repeated melting and solidification cycles leads to the generation of high magnitude residual stresses. These residual stresses can be detrimental both during manufacturing of components and in subsequent application. Therefore, a deep understanding of the influence of process parameters on the residual stresses are crucial for efficient manufacturing and safe application. The experimental characterization of these residual stresses is therefore crucial and can provide a reliable baseline for simulations of both the process and applications.

Diffraction-based methods for residual stress analysis using penetrating neutrons and high energy X-rays enable

non-destructive spatially resolved characterization of both surface and bulk residual stresses. However, the unique microstructural features inherent to the process can challenge some of our assumptions when using these methods. These challenges include the determination of a stress-free reference, the use of correct elastic constants (both SCEC and DEC) and the influence of surface roughness, texture, and porosity on residual stresses.

This presentation will detail recent insights and recommendations for the characterization of residual stresses in a range of PBF-LB/M metallic alloys (Fe, Ni, Al and Ti) [1-6].

1. I. Serrano-Munoz, A. Ulbricht, T. Fritsch, T. Mishurova, A. Kromm, M. Hofmann, R.C. Wimpory, A. Evans, G. Bruno, *Advanced Engineering Materials* 23(7) (2021).
2. I. Serrano-Munoz, A. Evans, T. Mishurova, M. Sprengel, T. Pirling, A. Kromm, G. Bruno, *Advanced Engineering Materials* 24(6) (2021).
3. I. Serrano-Munoz, T. Fritsch, T. Mishurova, A. Trofimov, D. Apel, A. Ulbricht, A. Kromm, R. Hesse, A. Evans, G. Bruno, *Journal of Materials Science* 56(9) (2020) 5845-5867.
4. T. Mishurova, K. Artzt, J. Haubrich, S. Evsevleev, A. Evans, M. Meixner, I.S. Munoz, I. Sevostianov, G. Requena, G. Bruno, *Metallurgical and Materials Transactions A* 51(6) (2020) 3194-3204.
5. J. Schroder, A. Evans, V. Luzin, G. Abreu Faria, S. Degener, E. Polatidis, J. Capek, A. Kromm G. Dovzhenko & G. Bruno, *J. Appl. Cryst*. 56, 1076-1090.
6. I. Roveda, I. Serrano-Munoz, T. Mishurova, M. Madia, T. Pirling, A. Evans, M. Klaus, J. Haubrich, G.Requena and G. Bruno, *Journal of Materials Science* 2022, **57**(48), pp. 22082–22098.

S5 - 6

HYDROGEN INTERACTION WITH ADDITIVELY MANUFACTURED STEELS CHARACTERIZED BY *IN-SITU* SYNCHROTRON X-RAY DIFFRACTION

Nicole Ofner[1*], T. Pogrielz[1], S. Bodner[1], C. Turk[2], C. Aumayr[2], L. Wu[3], J. Keckes[1]

[1]Montanuniversität Leoben, Department of Materials Science, A-8700 Leoben, Austria
[2]voestalpine Böhler Edelstahl GmbH & Co KG, A-8605 Kapfenberg, Austria
[3]voestalpine Additive Manufacturing Center GmbH, D-40667 Meerbusch, Germany
[*]nicole.ofner@unileoben.ac.at

In light of the growing interest in both hydrogen as a sustainable energy solution and hydrogen embrittlement of metals, the aim of the contribution is to analyse hydrogen interactions with additive manufactured (AM) components. For this purpose, two Chromium alloyed steels, further referred to as alloy A and B, with differing austenite and δ-ferrite contents, were selected for analysis in the as-built condition directly after the printing process. Laser beam powder bed fusion was used to successfully fabricate fully dense, crack-free specimens of both alloy systems. The additively manufactured specimens underwent a comprehensive characterization process, including laboratory X-ray diffraction (XRD), light microscopy, scanning electron microscopy, electron backscatter diffraction (EBSD), and hardness measurements. This provided an in-depth understanding of the microstructure and phase occurrences within the specimens as results of different chemical compositions. XRD and EBSD experiments revealed that alloy A had an austenite/δ-ferrite ratio of 80:20, displaying a typical AM microstructure with small δ-ferritic grains. In contrast, alloy B exhibited a ratio of 20:80, deviating from the typical AM microstructure and featuring larger δ-ferritic grains. Notably, hardness values in the as-built condition decreased with increasing ä-ferrite content, providing valuable insights into the mechanical properties of the investigated alloys.

As a next step, both AM specimens were charged with hydrogen and the different response of both alloys due to the varying austenite/δ-ferrite contents was evaluated. For this purpose, in-situ high-energy synchrotron XRD experiments coupled with electrolytic charging were conducted at the P07B beamline Petra III at DESY in Hamburg. The collected two-dimensional diffraction patterns were used to evaluate changes in lattice parameters and residual stresses within the two sample types. These changes occurred in both δ-ferritic and austenitic phases, but were strongly phase dependent.

Through these comprehensive characterizations, this study provides valuable insights into the influence of hydrogen embrittlement on multi-phase AM steels. This understanding is essential for addressing the practical implications of hydrogen embrittlement in AM components and promoting the utilization of hydrogen in modern industrial applications.

Session VI - Electromagnetic Methods and Steel

S6 - 1

STRESS ASSESSMENT FROM INCREMENTAL PERMEABILITY MEASUREMENTS

Eric Wasniewski[1,2,3,5], Laurent Daniel[2,3], Benjamin Ducharne[4,5], Fan Zhang[1]

[1]*Cetim, 52 avenue Félix Louat 60300 Senlis, France*
[2]*Université Paris-Saclay, CentraleSupélec, CNRS, Laboratoire de Génie Électrique et Électronique de Paris, 91192, Gif-sur-Yvette, France*
[3]*Sorbonne Université, CNRS, Laboratoire de Génie Électrique et Électronique de Paris, 75252, Paris, France*
[4]*Univ Lyon, INSA Lyon, LGEF EA682, 69621 Villeurbanne, France*
[5]*ELyTMaX IRL3757, Univ Lyon, INSA Lyon, Centrale Lyon, Université Claude Bernard Lyon 1, Tohoku University, Sendai 980-8577, Japan*

Incremental permeability measurements are a part of electromagnetic non-destructive testing (NDT), employed to characterize industrial components and assess cementation depth, hardness, or residual stresses. Residual stresses play a pivotal role in determining the performance, integrity, and service life of structural steels. A precise evaluation of internal stresses enables the anticipation of potential breakdown and degradation, averting disastrous consequences.

In the first part of the study, we investigate the change of magnetic properties of a specific type of steel as a function of stress. The second part introduces a model to predict these changes.

1. Introduction

Stress in industrial parts can make them wear out faster. Methods like X-Ray, drilling holes, or contouring can be used to evaluate stress, but they can be expensive or are not suitable for production monitoring. Another way of assessing stress, for magnetic materials, is to monitor their magnetic signature. This study investigates how a certain kind of stress affects magnetic signals, specifically the magnetic incremental permeability (MIP) [1].

2. Incremental permeability measurements on FeSi GO steel sheets.

2.1 Incremental permeability

As defined in the German standard [2], the Magnetic Incremental Permeability (or MIP) is defined as the slope of inner asymmetric loops (Figure 1). These loops, also called minor cycles, are obtained when the tested material is exposed to the superimposition of two magnetic loadings:

1. A low-frequency (quasi-static), high amplitude magnetic excitation, that provides a bias magnetization,
2. A high-frequency, low amplitude magnetic excitation, allowing the measurement of the relative magnetic incremental permeability μ_{MIPr}.

1.1 Experimental set-up

In this study, Iron-Silicon Grain Oriented (FeSi GO) laminated sheets, submitted to specific thermal treatment to induce grains of exceptional size (of the order of centimeters), were used. All samples were taken from the same batch and cut using electrical discharge machining (EDM) at different angles from the rolling direction (0°, 30°, 45°, 54.7°, 60°, and 90°). For each angle, Magnetic Incremental Permeability (MIP) and B(H) curve measurements under various levels of tension (0, 50, 100, 150 and 200 MPa) were conducted.

2. Numerical model – Multiscale model

The development of accurate models for magneto-mechanical effects is key to the evaluation of residual stresses from magnetic measurements. In this study, a multiscale model

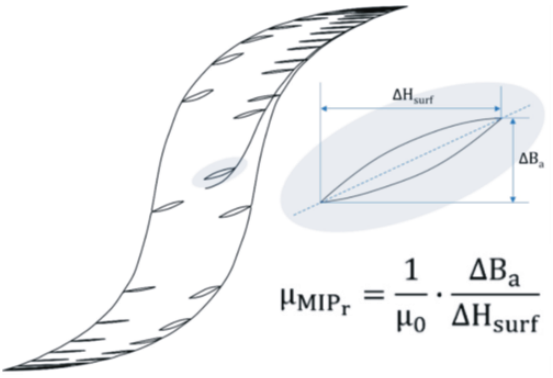

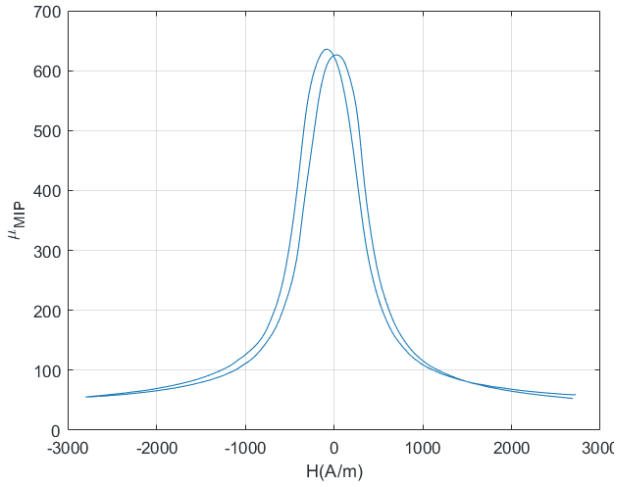

Figure 1. a) MIP Illustration and definition of MIP and b) example of incremental permeability measurement.

[3] was extended to model MIP. For this purpose, it is assumed that stress impacts MIP and differential permeability in similar ways.

3 Conclusion

The results a significant dependence of MIP on both orientation and amplitude of stress. A model of stress-dependent MIP has been developed to capture such effects.

References

1. B. Toutsop, B. Ducharne, M. Lallart, L. Morel et P. Tsafack, "Characterization of Tensile Stress-Dependent Directional Magnetic Incremental Permeability in Iron-Cobalt Magnetic Sheet: Towards Internal Stress Estimation through Non-Destructive Testing," Sensors, vol. 22, p. 6296, 2022.
2. DIN 1324, Deutsches Institut für Normung e.V.: Elektromagnetisches Feld, DIN, Éd., Berlin, 2017.
3. L. Daniel, O. Hubert, N. Buiron et R. Billardon, Reversible magnetoelastic behavior: A multiscale approach, vol. 56, J. Mech. Phys. Solids, 2008, pp. 1018-1042.

S6 - 2

CHARACTERIZATION OF THE SOLIDIFICATION STATE OF WELDED COLD-FORMED STEELS USING X-RAY DIFFRACTION

Th. Nitschke-Pagel[1], M. Dadkhah[1], J. Gibmeier[2], M. Zürn[2]

[1]Institut für Füge- und Schweißtechnik, TU Braunschweig, Germany
[2]Institut für angewandte Materialien, KIT, Germany

Material hardening that occurs during cold forming is an important tool for increasing the stability of car body components. For this reason, different types of steel with increased strengthening potential have been developed in recent decades. A general problem occurs, if cold-formed components are joined by welding process. Due to the applied thermal loads in the welded zones the hardening condition in the weld zone is worsened or completely neutralized due to recrystallisation and recreation and makes the use of enhanced steel qualities less useful.

Studies on steels with very different hardening potential are intended to show the connection between hardening caused by forming and thermally induced softening. Here the solidification state is characterized using conventional hardness tests and microindentation tests to determine force penetration curves. The hardness tests are compared

Figure 1. Comparison of hardness distributions and strengthening parameters obtained by diffraction line profile analysis of mild steel S355MC and high-strength TWIP-steel.

with results of a systematic analysis of measured X-ray interference lines using X-ray interference line profile analysis. The results show that the measurement methods used enable detailed statements to be made about the hardening condition after cold forming and the changes in the weld seam environment. The profile analyzes provide a refined view on the remaining dislocation density, domain size and micro-residual stresses. The derived integral widths can be correlated very well with measured mechanical hardness distributions and used to interpret the relationships between strain- and transformation-induced hardening, deformation-induced retained austenite transformation and thermally induced softening.

S6 - 3

RESIDUAL STRESSES IN STEEL BARS QUENCHED WITH WATER IMPINGING JET QUENCHING TECHNIQUE

P. Romanov[1,2], A. Jahedi[3], G. Gebeyaw[2], A. Carlestam[4], R. Kristensen[5], B. Moshfegh[2,6], V. Norman[1], R. Peng[1], M. Calmunger[1,2]

[1]Division of Engineering Materials, Department of Management and Engineering, Linköping University, SE-581 83 Linköping, Sweden
[2]Division of Building, Energy and Environmental Engineering, Department of Technology and Environment, University of Gävle, SE-801 76 Gävle, Sweden
[3]Ericsson AB, SE-164 40 Kista, Sweden
[4]SSAB Special Steel, SE-613 80 Oxelösund, Sweden
[5]Outokumpu Stainless AB, Jannelundsvägen SE-693 81 Degerfors, Sweden
[6]Division of Energy Systems, Department of Management and Engineering, Linköping University, SE-581 83 Linköping, Sweden
pavel.romanov@liu.se

Quenching of steel products from high temperatures is traditionally done by immersing them into a quenching medium which provides rapid cooling. However, depending on the type of steel and the dimensions of the product different cooling rates are required to obtain the desired effect. Furthermore, rapid cooling can result in undesired residual stresses due to thermal expansion and eventual phase transformations [1]. To avoid it the cooling rates during quenching must be accurately measured and controlled, and their effect on the arising residual stresses must be thoroughly studied.

A newly developed test rig for Impinging Jet Quenching Technique is used in this study to experimentally obtain different quenching scenarios for solid cylindrical carbon steel bars. The technique was successfully used for quenching of steel plates and hollow cylinders in previous studies [2-4]. Furthermore, a comprehensive quenching model is created to simulate the ongoing processes, including phase transformations, and to predict the resulting properties, microstructures, and residual stresses. The effect of steel properties on evolution of residual stresses is also demonstrated using simulation. Validation of the model is done through hardness measurements, optical microscopy, and residual stress analysis using X-ray diffraction method (XRD).

Microstructure and hardness measurements correlate well with the simulation results, clearly showing the effect of different quenching scenarios. Residual stresses of the bars obtained from simulations and XRD measurements follow the same trend and being compressive on the surface. The effect of carbon steel properties and the effect of surface cooling rates on the temperature evolutions and surface residual stresses, as well as the challenges of sample preparation affecting the residual stresses are brought up and discussed in this work.

1. A. Samuel, K. N. Prabhu, *Journal of Materials Engineering and Performance.*, **31**, (2022), 5161-5188.
2. M. Jahedi, *Experimental and Numerical Investigation of the Quenching Process on Rotary Hollow Cylinder by Multiple Impinging Jets*. Gävle: Gävle University Press, 2021.
3. P. Romanov, M. Jahedi, A. Petersson, B. Moshfegh, M. Calmunger, *Procedia Struct. Integr.*, **43**, (2023), 154-159.
4. P. Romanov, A. Jahedi, A. Bäckström, B. Moshfegh, I. Kuběna, M. Calmunger, *steel Res. Int.*, **95**, (2024).

S6 - 4

STRESS-CONCENTRATION BEHAVIOR IN SEVERAL DEFORMATION MODES SUSCEPTIBLE TO HYDROGEN EMBRITTLEMENT

Hyeonil Park[1], Dongjun Lee[1], Jonghwa hong[1], Yongnam Kwon[1], Sangcheon Lee[2], Jinwoo Lee[3]

[1]Korea Institute of Materials Science, 797, Changwon-daero, Seongsan-gu, Changwon-si, Gyeongsangnam-do, 51508, Republic of Korea
[2]Hyundia Motor Company, Hyundaiyeonguso-ro, Namyang-eup, Hwaseong-si, Gyeonggi-do, 18280, Republic of Korea
[3]University of Ulsan, 93, Daehak-ro, Nam-gu, Ulsan, Republic of Korea
hipark@kims.re.kr

In recent years, hydrogen has been attracting attention as a future energy source due to the global climate crisis and the active promotion of carbon neutrality policies. However, in the case of metallic materials, when exposed to a hydrogen atmosphere, hydrogen diffuses into the crystal structure of the metal, weakening the interatomic bonding, resulting in hydrogen embrittlement, which in turn deteriorates mechanical properties. Hydrogen embrittlement is caused by a complex interaction of environmental, material, and stress factors. Among these, stress-induced internal defects create an environment where hydrogen is easily adsorbed. In particular, high-strength steel sheets are generally more susceptible to hydrogen embrittlement due to their higher strength can cause larger stress during forming.

In this study, as part of the development of evaluation method and safety management for hydrogen embrittlement of high-strength steel sheets, we analyzed and predicted the stress concentration behavior that occurs during forming and derived its correlation with hydrogen embrittlement. The materials utilized in the tests were 1.2GPa and 1.5GPa-grade high-strength steel sheets. To evaluate the mechanical properties, which have different vulnerabilities depending on the deformation mode, 4-point bending tests, open hole tensile tests, and deep drawing tests were performed. The stresses generated in the material depending on the applied load were experimentally estimated, and they were predicted through finite element simulation to analyze the stress concentration behavior that occurs in several deformation modes that can be vulnerable to hydrogen embrittlement during the forming of high-strength steel sheets.

1. A. Del-Pozo, J. C. Villalobos, S. Serna, *Current Trends and Future Developments on (Bio-) Membranes*, **70**, (2020), 139-168.

This study was financially supported by the private consignment project (PICO350) funded by the Hyundai Motor Company (HMC), Republic of Korea.

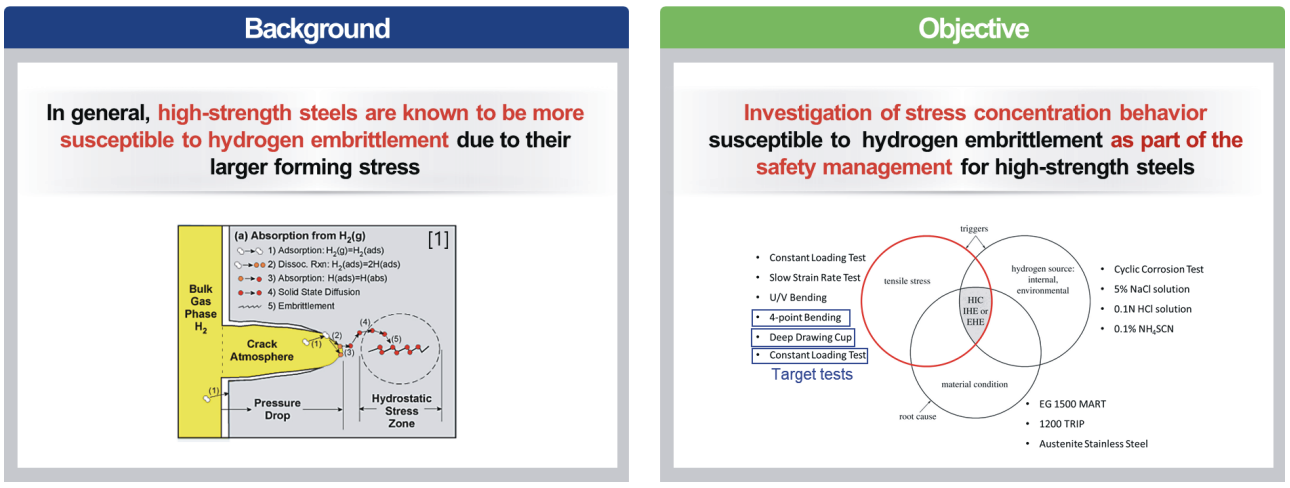

Figure 1. Background and objective of this research.

S6 - 5

TIME- AND DEPTH-RESOLVED CHARACTERIZATION OF HYDROGEN DIFFUSION INTO DUPLEX STEEL: LATTICE SWELLING AND STRESS EVOLUTION

T. Pogrielz[1], M. Eichinger[2], A. Weiser[3], J. Todt[1], J. Keckes[1], Norbert Schell[4]

[1]*Department of Materials Science, Chair of Materials Physics, Montanuniversität Leoben, 8700 Leoben, Austria*
[2]*Chair of General and Analytical Chemistry, Montanuniversität Leoben, 8700 Leoben, Austria*
[3]*Institute of Physics of Materials, AS CR, 61662 Brno, Czech Republic*
[4]*Institute of Materials Research, Helmholtz-Zentrum Geesthacht, Geesthacht, Germany*
thomas.pogrielz@unileoben.ac.at

Amidst the increasing enthusiasm for hydrogen as a sustainable energy solution across diverse industries and the formidable challenge posed by hydrogen embrittlement to reliability, gaining a comprehensive understanding of the intricate interplay between hydrogen and materials becomes imperative.

This contribution will present results from in-situ high-energy synchrotron X-ray diffraction experiments coupled with electrolytic charging of duplex steel with comparable ferrite and austenite phase fractions of various microstructures. The investigations performed at the high-energy materials science (HEMS) beamline P07B of the Petra III synchrotron radiation source were focused on examining the phase-selective swelling of crystal structures and characterizing the depth- and time-resolved evolution of in-plane stresses concerning crystallite size (Figure 1). For this purpose, a dedicated electrolytic cell was developed for the beamline. This cell employs a three-electrode setup, facilitating *in-situ* hydrogen charging based on 0.5M H_2SO_4 electrolyte. The double-walled polymer cell was kept the temperature of 53 °C constant over the experiment. Throughout the charging process spanning several hours, recurrent line scans were performed at 10 µm intervals, commencing at the surface and extending to a depth of 500 µm within the specimen. The line scans were conducted with a beam size of 500 x 10 µm, and a beam energy of 87.1 keV.

Commencing with the as-processed state, the material shows that sustained charging at constant current density induces substantial expansion specifically within the austenitic crystal structure, accompanied by minimal alterations in the lattice parameter of the ferrite. Furthermore, varying levels of compressive stresses emerge in both phases within the surface region of the sample.

Through the implemented modifications to the charging process and material's microstructure, charging could, for the first time, be documented based on local lattice changes in the ferritic phase. Furthermore, the charging and discharging processes were investigated, revealing intriguing near-surface effects. These observations suggest that hydrogen stored deeper within the material experiences a lower discharge potential compared to hydrogen located near the surface.

Once again, this experiment affirms the potential of the applied methodology and expands the material science understanding of hydrogen diffusion in steels.

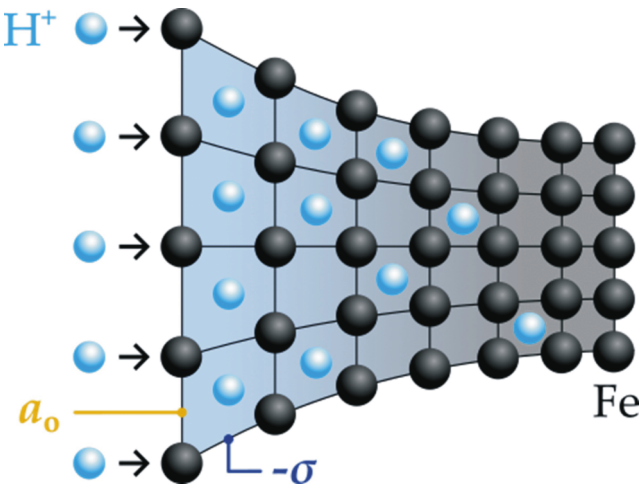

Figure 1. Illustration depicting the atomic lattice structure of a material subjected to electrolytic hydrogen charging, along with the ensuing gradients of lattice swelling and stresses between the free surface (left) and the bulk (right).

S6 - 6

THE CONTRIBUTION TO COMPLEX EVALUATION OF SURFACE INTEGRITY USING INSTRUMENTAL METHODS

Jiri Malec[1], Filip Cervinka[1], Aki Sorsa[2], Suvi Santa-aho[3] and Pavel Sandera[4]

[1]PCS, Department of Analytical Services, Zdar nad Sazavou, Czech Republic
[2]Environmental and Chemical Engineering, University of Oulu, Oulu, Finland
[3]Material Science and Environmental Engineering, Tampere University, Tampere, Finland
[4]Mechanical Engineering, Technical University of Brno, Czech Republic
j.malec@pcs.cz

Machinery generally uses frequently hard steels preciously machined. Parallel to proper size, surface hardness and general roughness some other parameters covered to complex term “surface integrity” are used to describe the behaviour of part in use. Due to fatigue life indirect description some other parameters sometimes summarized below the complex term “surface integrity” are used. For those purposes parameters mined from Barkhausen Noise Analysis (BNA), Residual Stress (RS) determination such as residual stress profiles are topical. This RS profiles can be used for calculation of Sum of Effective Residual Stresses (SERS). Paper introduces new parameter called Effective Residual Stresses Integral (ERSI) trying to describe plot of residual stress below the surface. In experimental part based on carburized steel samples some comparison of parameters based on BNA, RS tests, SERS and ERSI is presented. In this case surface integrity can be describe in terms of effective surface damage even in physical reasonable scale energy per square (Jm-2) forgetting different arbitrary units.

Session VII - Electron Microscopy, DIC, diffraction

S7 - 1

MICROSCALE RESIDUAL STRESS DISTRIBUTION INDUCED BY ABRASIVE WHEEL CUTTING OF Ti-6Al-4V

Akshay Mundayadan Chandroth, Marc Seefeldt, Joris Everaerts

Dep. of Materials Engineering, KU Leuven, Kasteelpark Arenberg 44 bus 2450, 3001, Leuven, Belgium
akshay.chandroth@kuleuven.be

Residual stresses in titanium alloys can have a significant impact on their mechanical performance. Understanding these stresses is critical in several applications, such as aerospace components and biomedical implants, because they affect the fatigue life of the manufactured components [1]. For certain components, metal cutting is a necessary step in the fabrication process. However, cutting techniques such as abrasive wheel sectioning, which is widely used for metal cutting, apply a significant mechanical force to the cut surface. This causes plastic deformation of the surface layers, resulting in residual stresses being developed underneath the surface. The development of compressive macroscale residual stresses below the cut surface has been reported for Ti-6Al-4V[2]. However, microscale residual stresses after cutting have not yet been studied, even though it is known that these can deviate significantly from the macroscale value, especially for materials with pronounced elastic-plastic anisotropy at the single crystal level such as α titanium [3]. In this study, we investigate near-surface microscale (Type II) residual stress variation in Ti-6Al-4V experimentally after sectioning with a silicon carbide abrasive wheel. Residual stress measurements were performed on cross-sections of cut bar specimens using the Focused Ion Beam - Digital Image Correlation (FIB-DIC) ring-core milling technique (see Figure 1a) [4]. This technique enabled evaluation of residual stresses in a gauge volume that is smaller than the average grain size of the material (approximately 11 µm) [5]. In contrast to previous studies, a wide range of both compressive and tensile microscale residual stresses were observed beneath the cut surface, which is presumably the result of type II residual stress variation (see Figure 1b). The dispersion in the observed values was highest close to the surface and decreased to a baseline range of ±200 MPa in the bulk of the material. An Electron Backscattered Diffraction (EBSD) analysis was performed on some of the measured points of interest to determine the local crystallographic texture of the measured region (see Figure 1c). The link between the accumulation of tensile and compressive residual stresses in different grains and their orientation with respect to the loading direction was investigated in order to explain the wide range of observed residual stress values. The presence of local near-surface tensile residual stresses after cutting has potential implications on fatigue crack initiation mechanisms.

1. P. J. Withers and H. K. D. H. Bhadeshia, "Residual stress. Part 2 - Nature and origins," *Mater. Sci. Technol.*, vol. **17**, no. 4, pp. 366-375, Apr. 2001, doi: 10.1179/026708301101510087.
2. E. Abboud, "Characterization of Machining-Induced Residual Stresses in Titanium-Based Alloys," McGill Univ., 2015, [Online]. Available: https://escholarship.mcgill.ca/concern/theses/th83m2360.
3. J. Chen, Z. Wang, and A. M. Korsunsky, "Multiscale stress and strain statistics in the deformation of polycrystalline alloys," *Int. J. Plast.*, vol. **152**, p. 103260, May 2022, doi: 10.1016/j.ijplas.2022.103260.
4. A. M. Korsunsky, M. Sebastiani, and E. Bemporad, "Residual stress evaluation at the micrometer scale: Analysis of thin coatings by FIB milling and digital image correlation," *Surf. Coat. Technol.*, vol. **205**, no. 7, pp. 2393-2403, Dec. 2010, doi: 10.1016/j.surfcoat.2010.09.033.
5. J. Everaerts, E. Salvati, F. Uzun, L. Romano Brandt, H. Zhang, and A. M. Korsunsky, "Separating macro- (Type I) and micro- (Type II+III) residual stresses by ring-core FIB-DIC milling and eigenstrain modelling of a plastically bent titanium alloy bar," Acta Mater., vol. 156, pp. 43-51, Sep. 2018, doi: 10.1016/j.actamat.2018.06.035.

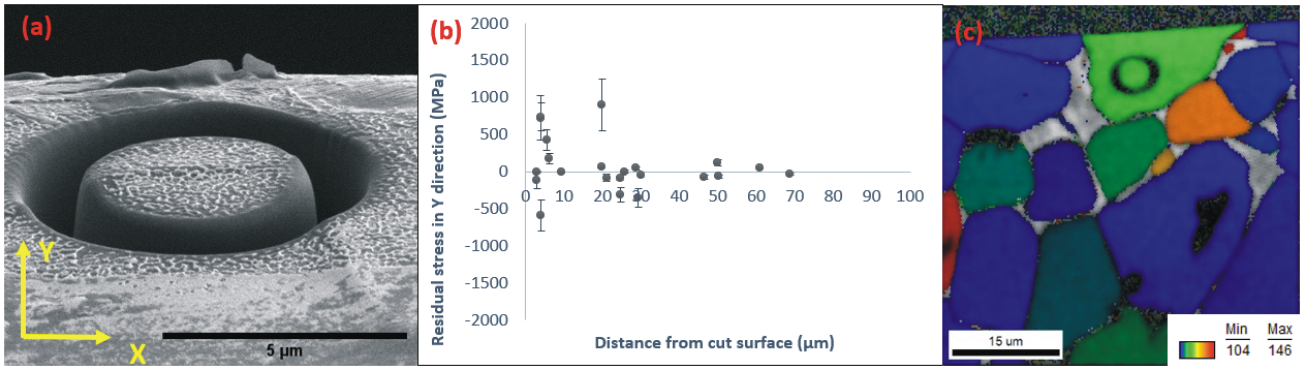

Figure 1. (a) FIB-DIC ring-core milling; (b) Residual stress values in the Y direction (perpendicular to the cut surface) versus distance from the cut surface; (c) Map obtained via EBSD after FIB-DIC milling, showing the local variation of Young's modulus (GPa) in the Y direction close to the cut surface.

S7 - 2

MICROSTRUCTURE AND DEFORMATION STATE IN ROTARY SWAGED COPPER

J. Kopeček[1], D. Šimek[1], P. Veřtát[1], A. Ubaid[1], M. Benč[2], S. Čech[2], L. Kunčická[2], R. Kocich[2]

[1]FZU – Institute of Physics of the Czech Academy of Sciences, Praha, Czech Republic
[2]Faculty of Materials Science and Technology, VŠB–Technical University of Ostrava, Ostrava-Poruba, Czech Republic
kopecek@fzu.cz

Rotary swaged copper and its composites with nanocrystalline oxides are prepared to improve mechanical properties of conventionally annealed electrotechnical material and preserve its good electric conductivity. The work is inspired by deformation procedures creating fine microstructure with high number of twin boundaries [1]. Despite obeying nanostructure, we created highly textured microstructure with excellent conductivity just by rotary swaging. Further annealing allows variation of microstructure due to the weakening of texture and decrease of deformation energy stored in material.

The set of pure copper bars was prepared by rotary swaging with different final diameter from 10 to 20 mm starting from original 50 mm bars [2]. The microstructure was investigated by both electron back-scattered diffraction method (EBSD) in scanning electron microscope (SEM) (Tescan FERA 3 and EDAX DigiView V) and X-ray diffraction (PANalytical X'Pert PRO). The residual stresses were evaluated from Williamson-Hall plots´ and corrected for Schmidt factor in respective crystallographic planes.

The two effects are observed in rotary swaged samples: the increasing amount of stored deformation with increasing diameter reduction, which can be attributed to dislocation and hydrostatic contribution due to the deformation in constrained environment. The hydrostatic contribution disappears in annealed samples, but dependence on reduction rate is preserved for all annealing procedures.

The observed XRD and EBSD measurements are correlated with TEM investigation (FEI Tecnai TF20 X-Twin) as the twins were expected in annealed samples.

1. L. Lu, Y. Shen, X. Chen, L. Qian, K. Lu, *Science* **304** (2004) 422.
2. J. Kopeček, L. Bajtošová, P. Veřtát, D. Šimek, *Materials*, **16** (2023), 5324.

We acknowledge Czech Science Foundation project 22-11949S and CzechNanoLab Research Infrastructure (LM2023051) by MEYS CR for support.

S7 - 3

EXPERIMENTAL STUDY AND MODELLING OF THE EFFECT OF SMAT TREATMENT ON NICKEL-BASED SUPERALLOYS

A. Garambois[1], Q. Barrčs[1], Y. Renollet[1], P. Kanouté[1], L. Toualbi[1], D. Retraint[2]

[1]ONERA Châtillon, France
[2]LASMIS, University of Technology of Troyes, France
anna.garambois@onera.fr

Mechanical surface treatments are widely used in the aerospace industry to improve the surface properties and delay fatigue crack initiation in critical parts, such as turbine disks. Surface Mechanical Attrition Treatment (SMAT) is a process that creates a nanocrystalline layer on the surface of treated mechanical parts in addition to superficial compressive residual stress and strain hardening. Previous studies have shown that SMAT can increase the yield strength [1], stress at failure, and improve the fatigue life [2] of metal parts by inducing severe plastic deformations at the surface of the material without altering its chemical composition [3] or core microstructure. The thermal and mechanical loads to which aeronautical components are subjected in service conditions induce relaxation of the residual stresses introduced into the material by the SMAT process. It is therefore essential to study this relaxation and the associated changes in material properties in order to assess the real impact of the SMAT process on the service life of these parts.

The work presented in this paper aims to characterise the gradient of material properties induced by the SMAT treatment and its evolution under thermomechanical stress. The residual stress profile was obtained using X-Ray Diffracton (XRD) coupled with material removal by electrolytic polishing, to make measurements at different depths in the material. Work hardening changes induced by SMAT was estimated from three variables: microhardness, crystal misorientation measured by EBSD, and full width at half maximum (FWHM) of XRD diffraction peaks. The study was conducted on Inconel 718, with two different sets of SMAT parameters. Figure 1 shows the local misorientation obtained by EBSD–KAM on two samples for conditions designated SMAT2 and SMAT3.

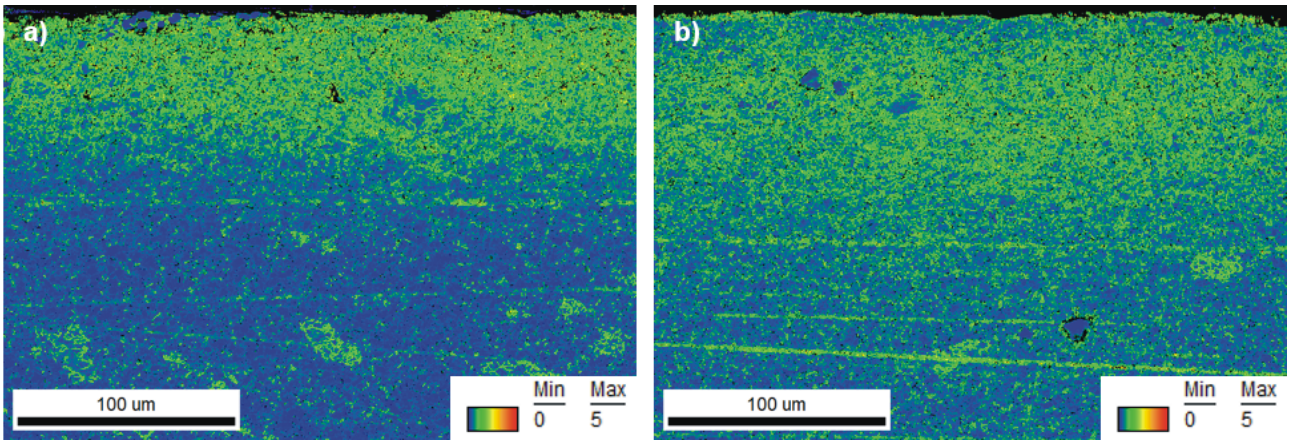

Figure 1. EBSD map of kernel average misorientation (KAM) of Inconel 718 treated with a) SMAT2 b) SMAT3

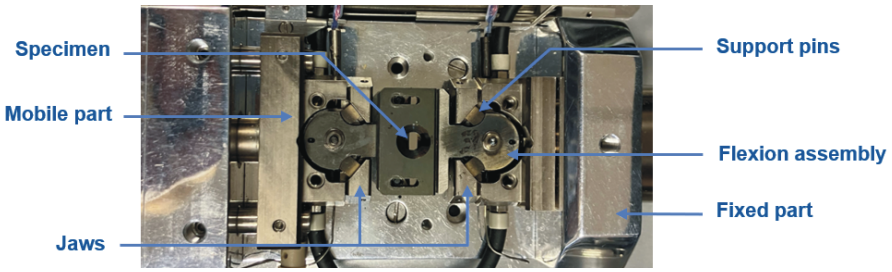

Figure 2. *In situ* SEM bending test setup.

As shown in Figure 1, the microstructural changes induced by the SMAT process are localised within the first few hundred micrometers of the sample surface and may impact the mechanical properties of the material under thermomechanical loading. In order to capture these evolutions at the appropriate scale, innovative characterization techniques, such as *in situ* SEM testing, are required. Combined with Digital Image Correlation (DIC), this technique allows access to the local strain fields of the specimen by calculating the displacements of each pixel between the reference image and the images of the deformed material taken during the test. The setup used is shown in Figure 2. Local changes in microstructure and mechanical parameters can be monitored using this experimental protocol, particularly when these tests are coupled with EBSD analysis.

In situ SEM 4-point bending tests were performed first at 20 °C on both untreated and SMAT2-treated samples, and then at 450 °C, using the natural microstructure of the material as a speckle pattern to identify the pixels of the image. The quality of the correlation is illustrated in Figure 3, with the map of the correlation coefficients obtained during a test. Figure 4 shows the force-deformation curves obtained for all tests on the surface of the material. These results show a delayed onset of plasticity in the SMAT treated material at 20 °C and 450 °C compared to the untreated material. In addition, the work hardening mechanisms appear to be significantly altered by the process.

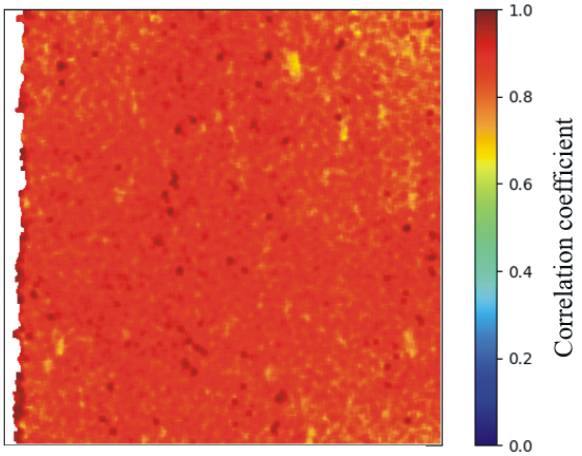

Figure 3. Correlation coefficient map obtained by DIC during *in situ* SEM testing on Inconel 718.

Simulations of these bending tests have been carried out considering the surface residual stress gradient in the specimen, based on the profiles determined by XRD. These simulations have been compared with the experimental results to assess the need to modify the hardening properties of the treated material in comparison to the untreated one. The aim is to build a model accounting for the cycling non-linear behaviour of the material for fatigue life time estimation.

1. S. Kumar, G. Sudhakar Rao, K. Chattopadhyay, G. S. Mahobia, N. C. Santhi Srinivas, et V. Singh, " Effect of surface nanostructure on tensile behavior of superalloy IN718 ", *Mater. Des.* 1980-2015, vol. 62, p. 76-82, 2014.
2. T. Roland, D. Retraint, K. Lu, et J. Lu, " Fatigue life improvement through surface nanostructuring of stainless steel by means of surface mechanical attrition treatment ", *Scr. Mater.*, vol. 54, no 11, p. 1949-1954, 2006.
3. F. A. Guo, N. Trannoy, et J. Lu, " Microstructural analysis by scanning thermal microscopy of a nanocrystalline Fe surface induced by ultrasonic shot peening ", *Superlattices Microstruct.*, vol. 35, no 3-6, p. 445-453, 2004.

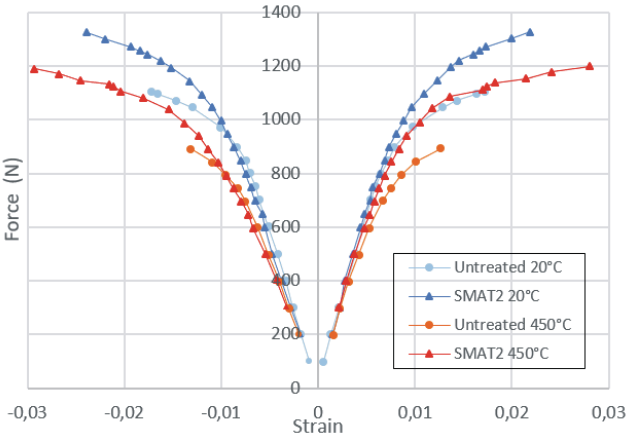

Figure 4. Results of *in situ* SEM 4-point bending tests on untreated and SMAT2-treated Inconel 718 samples.

S7 - 4

A NUMERICAL STUDY ON THE EFFECT OF INTERNAL RESIDUAL STRESS INDUCED BY SURFACE SEVERE PLASTIC DEFORMATION PROCESS ON MECHANICAL BEHAVIOR

Jong-Hwa Hong[1], Hyeonil Park[2], Yong-Nam Kwon[2], Dong Jun Lee[2,#]

[1]Department of Materials Processing, Korea Institute of Materials Science, 797 Changwondae-ro, Changwon, Gyeongsangnam-do 51508, Republic of Korea
[2]Aerospace Materials Center, Korea Institute of Materials Science, 797 Changwondae-ro, Changwon, Gyeongsangnam-do 51508, Republic of Korea
[#]djlee@kims.re.kr

Recent research revealed that although the surface severe plastic deformation (SSPD) process enhances mechanical properties through the formation of a fine grain reinforcement layer on the surface, it can concurrently result in a transient behavior at the early stage and a reduction in yield strength in the uniaxial tensile test. This is because the impact of the generated residual stress outweighs the strengthening effect of the surface layer formed by SSPD. The study analytically and numerically validated the presence of the transient behavior in the initial stage and the reduced yield strength, attributing this phenomenon caused by internal tensile residual stress, generated to maintain equilibrium. This presentation extends the previous research to the effect of internal residual stress on other mechanical behavior, fatigue crack propagation (FCP). To understand FCP, crack propagation behavior during the uniaxial tensile test is studied after the SSPD process. For the analysis, analytical and numerical models are developed using formulations and numerical simulation with the extended finite element method (X-FEM). This model aims to scrutinize the influence of residual stress imposed by the SSPD process on fatigue crack propagation behavior anticipating that this method will be a valuable tool for comprehending the effect of residual stress on fatigue crack propagation in the future.

1. Hong, J. H., Park, H., Kim, J., Seok, M. Y., Choi, H., Kwon, Y. N., & Lee, D. J. (2023). Effect of the residual stress induced by surface severe plastic deformation on the tensile behavior of an aluminum alloy. Journal of Materials Research and Technology, 24, 7076-7090.
2. P. J. Chupas, M. F. Ciraolo, J. C. Hanson, C. P. Grey, *J. Am. Chem. Soc.*, **123**, (2001), 1694.

S7 - 5

MULTISCALE MICROSTRUCTURE AND STRAIN CHARACTERISATION IN ALUMINIUM USING DARK-FIELD X-RAY MICROSCOPY

A. Cretton[1], A. Zelenika[1], S. Borgi[1], F. Frankus[2], F. B. Grumsen[2], C. Yildirim[3], C. Detlefs[3], G. Winther[2], H. F. Poulsen[1]

[1]Technical University of Denmark, Department of Physics, Kgs. Lyngby, Denmark
[2]Technical University of Denmark, Department of Civil and Mechanical Engineering, Kgs. Lyngby, Denmark
[3]European Synchrotron Radiation Facility, Grenoble, France
adacre@dtu.dk

This work present first results from the new dark field x-ray microscopy (DFXM) beamline at ID03 at ESRF. DFXM is akin to dark field TEM but applies to bulk samples. It allows for the creation of 3D visualisations of local orientations and strains in samples up to millimetre sizes with a spatial resolution of about 100 nm, angular resolution of 0.001°, and strain resolution of 10^{-4}. Hence, it allows characterization of microstructure and strain on three length scales: the continuum, inter- and intergrain grain length scale, simultaneously - in 3D, and as function of the applied strain. Initial experiments have been based on diffraction imaging based on a single reflection; plans are underway to extend this to three reflections to deepen the multi-scale analysis of hierarchical structures.

As examples I will present studies of the formation and refinement of dislocation cells in pure Al during tensile loading. Firstly, I will present statistics on 40,000 cells for a single crystal with along the tensile axis up to 4.6% applied strain. Next, I will show initial results on the strain and microstructure evolution for a (100) crystal up to 7 % strain.

Limitations and on-going developments of the method will be presented for discussion.

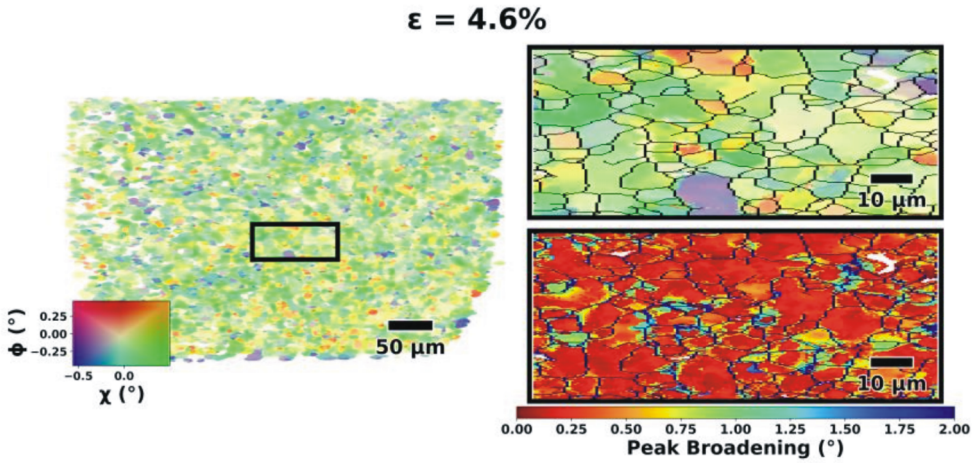

Figure 1. Orientation map with IPF colour code of aluminium sample deformed to ε = 0.046. Zoom in on region marked in on the left with misorientations above 0.4° as black lines. Corresponding peak broadening map, indicative of the local dislocation density and residual strain.

Session VIII - Ni-based and Light Metals

S8 - 1

FORMATION OF RESIDUAL STRESSES DURING QUENCHING OF Ti17 AND Ti-6Al-4V ALLOYS: INFLUENCE OF PHASE TRANSFORMATIONS

J. Teixeira[1,2], D. Maréchal[1,2], R. C. Wimpory[3], S. Denis[1,2], F. Lefebvre[4], R. Frappier[5]

[1]*Institut Jean Lamour, UMR 7198 CNRS – Univ. Lorraine, Nancy, France*
[2]*Laboratory of Excellence "Design of Alloy Metals for Low-mass Structures" (DAMAS), Univ. Lorraine, France*
[3]*Helmholtz-Zentrum Berlin für Materialien und Energie GmbH, Berlin, Germany*
[4]*CETIM, Senlis, France*
[5]*Mat-In-Meca, Sainte-Cécile, France*
julien.teixeira@univ-lorraine.fr

The sequences of thermomechanical processes applied to titanium alloys generally include several quenching operations, which give rise to the formation of residual stresses, including macroscopic or first order residual stresses. In titanium alloys, the internal stresses and the plastic deformations come in large part from the thermal gradients which are established inside the treated part during the cooling. Few studies (mostly on Ti-6Al-4V alloy and welding) investigated the possible effects of phase transformations, and there is currently no general agreement in literature on their magnitude. The present study aims at investigating further these effects by several means, in the case of quenching.

The formation of internal stresses during quenching of titanium alloys from the β phase field are investigated both experimentally and by simulation, in order to show the effects of phase transformations. Two titanium alloys are considered: the β-metastable Ti17 alloy and the α+β Ti-6Al-4V alloy. During the quench into water of laboratory scale samples (40 mm diameter cylinders), no phase transformations occurred in the Ti17 alloy because of its β-metastable character and the fast cooling: it thus remained in β state. However, β→α+β and β→α' phase transformations occurred in the Ti-6Al-4V sample. Both alloys were compared in order to highlight the effects of the phase transformations. Residual stresses were determined by neutron diffraction and by the contour method, and at the surface by the hole drilling method. A model for the coupled thermal, mechanical and metallurgical evolutions was established in order to simulate the quenching operations. The material model for the Ti17 alloy was established in a previous study [1]. Regarding the Ti-6Al-4V alloy, modelling approaches [2] and experimental data from literature [3] were utilized to build the material model.

From both experiment and simulation, it is found that the internal stress evolutions are governed by the thermal gradients for both the Ti17 and the Ti-6Al-4V alloys. After the quench, the cylinders show tensile residual stresses near the center and compressive stresses near the surface, according to the experiments. This is shown for instance in Fig. 1 for the Ti-6Al-4V alloy, which compares the axial residual stress profiles determined by the different methods, along the radius and inside the median plane. (The results for the Ti17 alloy are shown in reference [4]). The profiles of residual stress predicted by the simulation are compared to the experiment in Fig. 2. According to the

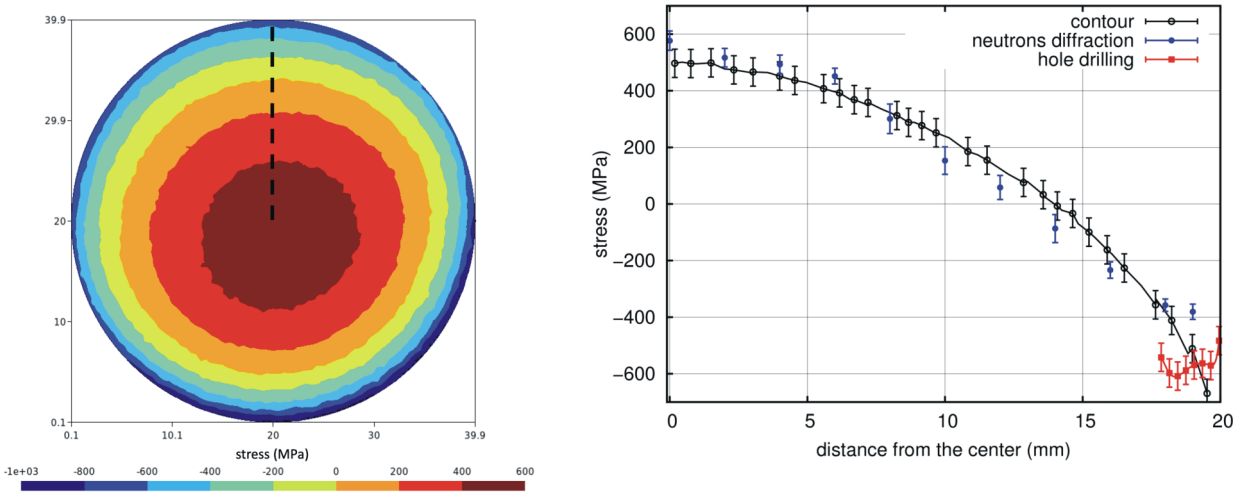

Figure 1. Ti-6Al-4V cylindrical specimen: a) Two-dimensional map of the axial residual stresses determined by the contour method in the median plane. b) Comparison between the axial residual stress profiles determined by the contour method (along the dashed line represented in a), by neutron diffraction and by hole drilling.

simulations, the residual stresses come from the plastic deformations induced by the thermal stresses during the quench. Hence on first analysis, the phase transformations have no significant impact on the internal / residual stresses, and this is due to the small deformation strains induced by the phase changes (volume change, phase transformation plasticity).

However, the simulations also show that accurate prediction of the phase transformation kinetics is necessary to predict the residual stresses values, in the Ti-6Al-4V alloy. When the β→α+β and β→α' occur during the cooling, this quickly strengthens the alloy and this puts an end to the accumulation of the plastic strains, which are at the origin of the residual stresses. As most plastic strains are cumulated at high temperature, and mostly when the alloy is still in β state, the thermomechanical model should also be established accurately over the temperature ranges in which there is a significant proportion of β phase.

1. J. Teixeira, B. Denand, E. Aeby-Gautier, S. Denis, *Materials Science and Engineering A*, **651**, (2016) 615.

2. A. Longuet, Y. Robert, E. Aeby-Gautier, B. Appolaire, J.F. Mariage, C. Colin, G. Cailletaud, *Computational Materials Science*, **46**, (2009), 761.

3. R. Julien, V. Velay, V. Vidal, Y. Dahan, R. Forestier, F. Rezad'-Aria, *International Journal of Mechanical Sciences*, **142-143**, (2018), 456.

4. J. Teixeira, D. Maréchal, R. C. Wimpory, S. Denis, F. Lefebvre, R. Frappier, *Materials Science and Engineering A*, **832**, (2022) 142456.

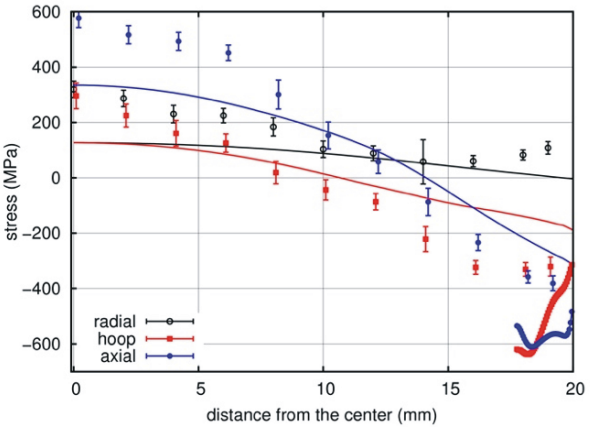

Figure 2. Residual stress radial profiles in Ti-6Al-4V sample median plane, determined experimentally from neutron diffraction (dots) and hole drilling method (bold lines). Calculated stress profiles (thin lines) obtained by numerical simulations. The latter show the average of stresses calculated in α and α' phases.

This work was supported by the French State through the program "Investment in the future" operated by the National Research Agency (ANR) and referenced by ANR-11-LABX-0008-01 (LabEx DAMAS). TIMET Savoie is gratefully acknowledged for providing both the Ti17 and the Ti-6Al-4V alloy materials, and for discussions with Yvon Millet. We wish to thank HZB for the allocation of neutron radiation beam time. The society Mat-in-Meca© is thanked for the residual stress determinations by the contour method.

S8 - 2

IN718 COLD GAS REPAIR SPRAY OF LARGE CAVITIES – INFLUENCE OF DIFFERENT GEOMETRIES ON RESIDUAL STRESS DISTRIBUTION

Florian Lang[1], Johannes-Christian Schmitt[2], Sandra Cabeza[3], Thilo Pirling[3], Robert Vaßen[2], Jens Gibmeier[1]

[1]*Institute for Applied Materials (IAM-WK), Karlsruhe Institute of Technology (KIT), Engelbert Arnold Str. 4, 76131 Karlsruhe, Germany*
[2]*Institute of Energy and Climate Research (IEK-1), Forschungszentrum Jülich GmbH, Wilhelm-Johnen-Straße, 52425 Jülich, Germany*
[3]*Institut Laue-Langevin (ILL), 71 Avenue des Martyrs, 38000 Grenoble, France*
Florian.Lang@kit.edu

Cold gas spraying (CGS) is an established thermal spraying process for coating substrates with similar or dissimilar materials. By using a high-pressure process gas flow, solid particles are accelerated to supersonic velocity and directed onto a substrate, where the particles then combine to form a closed coating. Compared to other thermal spraying processes, CGS is considered a low temperature process, as the deposition occurs not in a molten or gaseous state, but in solid state. The bonding of particles to the substrate takes place due to the high kinetic energy of the supersonic particles. When the accelerated particles hit the substrate, strong plastic deformations occur, which lead to a form-fit connection of the particles with the substrate [1]. Compared to conventional thermal spraying processes, CGS is more environmentally friendly, as the power requirement is lower, and toxic gases or chemicals are not necessary. The method is particularly suited for repair applications, since neither structural changes nor oxidation occur during the process [2]. The substrate surface is usually pre-treated by sandblasting in order to improve adhesion. Combined with the blasting effects of CGS, this usually results in compressive residual stresses close to the component surface, which are thought to have a positive influence on the wear and fatigue behaviour [3]. For comparable material combinations, Vaßen et al. found for instance axisymmetric compressive residual stresses in thin Inconel 718

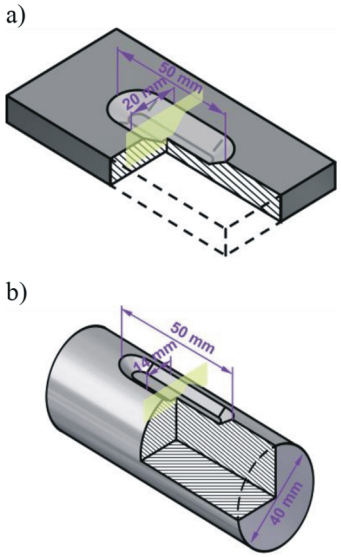

Figure 1. Schematic of the investigated flat (a) and cylindrical (b) geometries with a tapered cavity filled by means of cold gas repair spray. All dimensions given in mm.

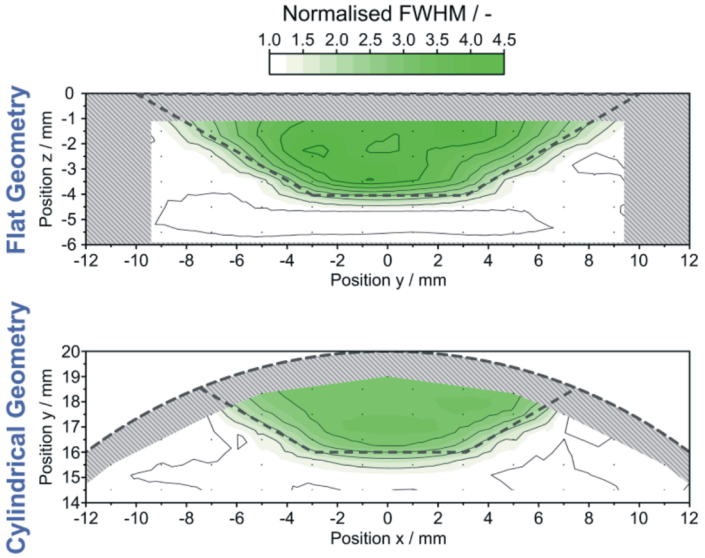

Figure 2. Results for the flat geometry (top) and the cylindrical geometry (bottom): Contour graphs of the normalised FWHM. The cross hatched areas represent the specimen. The dashed line represents the contour of the cavity. The black dots represent measurement locations.

coatings on Inconel 718 substrates produced by CGS. These are balanced by tensile residual stresses in the surrounding bulk material. In contrast, depending on the material pairing and process used, other thermal spray processes often lead to thermally induced tensile residual stresses [4].

With the desire for increased sustainability, it is both environmentally and economically advantageous to be able to successfully repair even major damage to, for example, turbine engine components made of Alloy 718, and to extend the life of such costly parts without having to replace the entire component. To investigate the suitability of the CGS process for the repair of large, near-surface damage in Alloy 718 components, flat sample geometries containing cavities with a depth of 4 mm, as shown in Figure 1a, were fabricated and investigated in a previous study [5]. In order to investigate the influence of the substrate geometry on the deposition quality and the resulting residual stress distribution, in a follow-up experiment cylindrical specimens with a diameter of 40 mm containing the repair site on the circumference were fabricated. Figure 1b) shows a schematic of the cylindrical sample geometry. Beside the sample geometry and its dimension, figure 1 indicate that the sidewalls of the cavities were tapered to facilitate gas flow and improve adhesion. The cavities were filled with Alloy 718 particles from CGS using two sets of processing parameters. This geometry results in a different constraint compared to the geometry used in the previous investigations due to the changed geometric boundary condition.

Non-destructive high resolution neutron diffraction experiments were performed on the as-sprayed samples using the SALSA instrument at the Institut Laue-Langevin (ILL) to determine the triaxial local residual stress state in the as-sprayed condition. As a result, 2D maps of the residual stress distributions over the cross-sectional area of the samples were determined in the centre of the cavities. Complementary laboratory X-ray diffraction (XRD) and incremental hole drilling analyses were carried out to provide additional near surface results. Knowledge of the residual stresses for the as-sprayed condition is essential for assessment of the process results, since not least the comparatively high process-related residual stresses can be associated with a potential for distortion of the component or can promote early failure of the repair zone. The results of the residual stress analyses indicate compressive residual stresses within the repaired process zone and compensating tensile residual stresses in the bulk material below the interface, while differences occur with respect to the sample geometry. To underline this, the contour plots in Figure 2 show the normalised full width at half maximum (FWHM) of the neutron diffraction lines for both the flat and cylindrical sample geometries. The FWHM is normalised to the average FWHM of the surrounding substrate material away from the interface. The significantly increased width of the diffraction lines in the filling indicates significant plastic deformation of the spray particles during CGS. This is corroborated by metallographic examination, which shows highly deformed particles within the repaired region.

1. V.K. Champagne Jr., et. al., *Practical Cold Spray*, (Cham: Springer), 2021.
2. H. Assadi, H.Kreye, F. Gärtner, T. Klassen, *Acta Mater.* **116**, (2016).
3. R. Singh, S. Schruefer, S. Wilson, J. Gibmeier, R. Vassen, *Surf. Coat. Technol.*, **350**, (2018).
4. R. Vaßen, J. Fiebig, T. Kalfhaus, J. Gibmeier, J. Kostka, S. Schruefer, *J. Therm Spray Tech*, **29**, (2020).
5. F. Lang, J.-C. Schmitt, S. Cabeza, T. Priling, J. Fiebeig, R. Vaßen, J. Gibmeier, in *Proceedings of the 10th International Symposium on Superalloy 718 and Derivatives,* edited by E. Ott et al. (Cham: Springer), 2023, pp. 739-753.

The authors would like to thank the German Research Foundation (DFG) for funding the project 452606919. The authors are grateful to the Institut Laue-Langevin for granting beamtime at the SALSA instrument and for their support.

S8 - 3

MICROSTRUCTURE AND MECHANICAL PROPERTIES OF NI-BASED POWDER METALLURGY SUPERALLOY TREATED BY SURFACE MODIFICATION PROCESSES

Dong Jun Lee[1], Yun-Ji Cho[1], Min-Jae Baek[1], Eun Yoo Yoon[2], Moo-Young Seok[1], Hyoenil Park[1], Hyunsung Choi[1], Kyung Su Kim[3]

[1]Aerospace Materials Center, Korea Institute of Materials Science, 797 Changwondaero, Changwon, Gyeongnam-do, Republic of Korea
[2]Department of Materials Processing, Korea Institute of Materials Science, 797 Changwondaero, Changwon, Gyeongnam-do, Republic of Korea
[3]FusionENG, 40 Omokcheon-ro 152beon-gil, Gwonseon-gu, Suwon-si, Gyeonggi-do, Republic of Korea
djlee@kims.re.kr

Nickel-base superalloys are the material for the gas turbine engines in the harshest operating conditions, specifically the turbine discs. In the early seventies, the powder-processed Ni-based superalloys were developed for use in high-performance aero engine discs due to more uniform composition, phase distribution, finer grain size, higher strength, reduced carbide segregation, and increased flexibility in alloy design. Ni-based superalloy powders are first consolidated into fully dense compacts by hot isostatic pressing (HIP). This superalloy exhibits excellent fatigue properties and creep resistance at high temperatures. However, because it is made from powder, micropores and prior particle boundaries exist inside. These defects cause lower fatigue and creep resistance. In this study, ultrasonic-nanycrystalline surface modification (UNSM) and laser shock peening (LSP), a process that artificially imposes residual stress on the surface, were applied to improve this problem. The surface-treated specimens were analyzed for microstructure, residual stress, and fatigue characteristics.

S8 - 4

RESIDUAL STRESS AND PRECIPITATION BEHAVIOUR DURING HEAT TREATMENT OF FGH96 ALLOY

Dingge Fan[1], Xiongxi Zhao[1], Jian Zhang[1], Jiantang Jiang*[1,2]

[1]School of Materials Science and Engineering, Harbin Institute of Technology, Harbin, 150001, China
[2]National Key Laboratory of Precision Hot Processing of Metals, Harbin Institute of Technology, Harbin, 150001, China
DinggeFan1@163.com

The impact of heat treatment on residual stress and precipitation behaviour in FGH96 alloy was investigated. Results obtained from the contour method for evaluating residual stress in FGH96 alloy demonstrate that aging conducted at 760 °C enhances mechanical properties and reduces residual stress levels. The size of secondary γ' precipitates gradually increases with prolonged aging duration. However, the increase in hardness of FGH96 alloy after a 1-hour aging period is found to be insignificantly significant, indicating a gradual decrease in the contribution of precipitate strengthening as the size of secondary γ' precipitates increases. The classical precipitation-strengthening models are utilized to calculate the optimal size of γ' precipitates (rw) in nickel-based superalloys. The size of the γ' precipitates in the bulk sample is found smaller than rw, which then guide the optimization of the heat treatment scheme through reducing the quenching rate. Minimized residual stress and optimized mechanical properties was achieved synergistically via the process optimization.

Full paper in ECRS-11 Conftool

S8 - 5

X-RAY DIFFRACTION ANALYSIS OF ADDITIVELY MANUFACTURED AlSi10Mg ALLOY

J. Čapek[1], K. Trojan[1], R. Halama[2], J. Hajnyš[2], N. Ganev[1], K. Kolařík[1]

[1]Czech Technical University in Prague; Trojanova 13, 120 00 Prague, Czech Republic
[2]VSB - Technical University of Ostrava; 17. listopadu 2172/15, 708 00 Ostrava - Poruba, Czech Republic
jiri.capek@fjfi.cvut.cz

Additive manufacturing, namely Selective Laser Melting (SLM) technology, is a promising metal powder consolidation method and offers outstanding parts production opportunities. It is based on selectively melting parts of a thin flat powder bed in layers using a scanning energy source to produce 3D parts. The intricacy of the SLM process results in the magnitude and orientation of residual stresses (RS) being highly dependent on laser power, scanning speed, scanning strategy, and other processing parameters [1].

The effect of RS manifests itself in different ways. In particular, high tensile RS can lead to deformation and subsequent cracks in printed parts, which can disrupt the overall strength of the part. They can also affect the geometry of the printed object. Some shapes and structures are more sensitive to RS than others, especially in the horizontal printing strategy. Generally, tensile RS in the sub/surface layer reduce mechanical as well as corrosion properties. The notch toughness, fatigue resistance and wear resistance properties are reduced too; moreover, such factors as crack propagation rate, corrosion cracking and intergranular corrosion are supported.

The initiation of fatigue cracks and their propagation play a significant role in fatigue properties with a strong dependence on surface roughness, microstructure parameters (dislocation density, crystallite size, microstrains), and RS [2]. In the study [3], the explicit correlation between the initialisation of surface fatigue cracks and its propagation with RS has been investigated using X-ray diffraction. It was found that not only RS but also the distribution of microstructure parameters plays a crucial role in fatigue. In a previous study [4], a correlation was observed between the relaxation of structure-sensitive characteristics and the formation of surface fatigue cracks for welded materials. The basis of this investigation will be applied to this contribution, which deals with the study of additively manufactured AlSi10Mg.

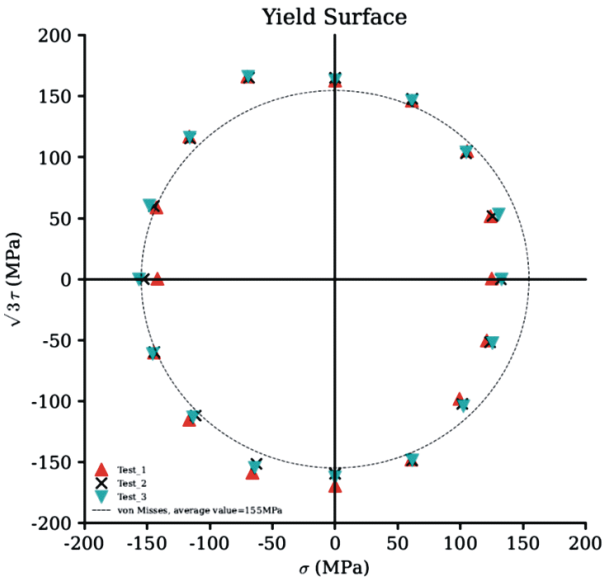

Figure 1. The size of the elastic region.

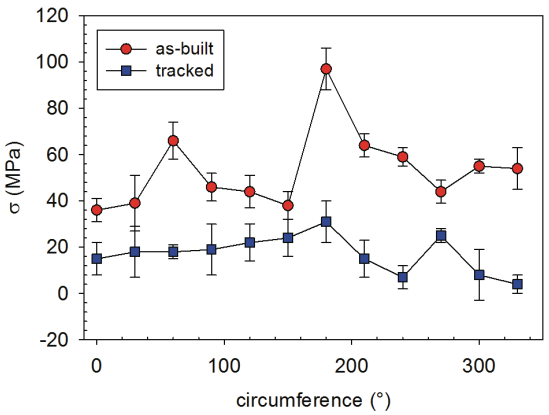

Figure 2. Comparison of residual stresses of tracked and as-built sample.

The measured data were fitted with the von Mises condition with a yield strength of an average value of 160 MPa (corresponding to 0.005% of plastic strain). The same value was evaluated from a tensile test. The yield strength (corresponding to 0.2% of the plastic strain) is given by around 255 MPa. Compared to the maximum value of RS, which is 100 MPa for the aluminium phase, it is possible to state that in some surface RS reach 63% of the yield strength and, therefore; 60 MPa of external tensile stress will result in plastic deformation. The higher yield strength in compression, which is obvious from Figure 1, is the confirmation of the tensile residual stress observed by XRD analyses. Nevertheless, the results from the Al phase are influenced by both Al in solid solution and eutectoid too, where one of the Al phases should be harder and, therefore; one Al phase should be elastic, and the second in the plastic region. The RS of Al phase were redistributed/reduced and homogenized their values; see Figure 2.

1. J. L. Barlett, X. Li, *Addit. Manuf.*, **27**, (2019), 131-149.
2. W. Schneller, M. Leitner, S. Pomberger, S. Springer, F. Beter, F. Grün, *J. Manuf. Mater. Process.*, **3**, (2019), 89.

3. J. Čapek, K. Trojan, J. Kec, I. Černý, N. Ganev, S. Němeček, *Mater.*, **14**, (2020), 131.

4. I. Černý, J. Čapek, J. Kec, K. Trojan, N. Ganev, S. Němeček, in *Comprehensive Structural Integrity*, edited by F. Aliabadi & W. Soboyejo (Elsevier Science), 2023.

Measurements were supported by the project 23-05338S of the Czech Science Foundation. The work of CTU staff was supported by the Grant Agency of the Czech Technical University in Prague, grant No. SGS22/183/OHK4/3T/14 and the Technology Agency of the Czech Republic No. TQ03000457.

S8 - 6

PLASTIC DEFORMATION STUDY FOR MAGNESIUM AZ31 USING NEUTRON DIFFRACTION DURING VARIOUS DIRECTIONS OF LOADING

P. Kot[1*], A. Baczmański[2], A. Ludwik[2], M. Wroński[2], S. Wroński[2], G. Farkas[3]

[1]*CoE NOMATEN, National Institute for Nuclear Research, A. Sołtana 7, 05-400 Otwock, Poland*
[2]*AGH University of Science and Technology, WFiIS, al. Mickiewicza 30, 30-059 Kraków, Poland*
[3]*Nuclear Physical Institute, ASCR, Hlavni 130, 25068 Řež, Czech Republic*
**przemyslaw.kot@ncbj.gov.pl*

In this work, a hot-rolled AZ31 magnesium alloy exhibiting a fibre texture with a strong (0001) base component was investigated. Stress measurements were made during compression along rolling direction (RDC), compression along normal direction (NDC) and loading in a direction deviated from the normal direction (ND) by 30° towards the rolling direction ND (later called Mg30), cf. Fig. 1. The experiment was carried out on a TKSN 400 (HK9) diffractometer at the Institute of Nuclear Physics in Řež (Czech Republic) using the angular dispersion method. The results of the crystallite group analysis [1] were compared with previous *in-situ* measurements using the time-of-flight (ToF, energy dispersion) technique [2]. A good agreement between the results was obtained.

The idea of measurement for a sample loaded in a direction tilted by 30° from ND (Mg30) is to meet the main assumption of the crystallite group method: the selected crystallite group should be dominant, because then the grains with the preferred orientation of the crystallite lattice have the greatest influence on the measured lattice deformations. The performed measurements confirmed the previously determined critical shear stresses (CRSSs) for the basal slip system [2]. The obtained results, i.e. the set of CRSS values for various slip and twinning systems, allowed for the unambiguous fitting of a self-consistent elasto-plastic model and the determination of slip hardening parameters. The fitted model results are consistent with the measured lattice strains and macroscopic stress-strain curves. Moreover, the model correctly predicts macroscopic curves measured ex-situ in different directions (see Fig. 1 and Fig. 2).

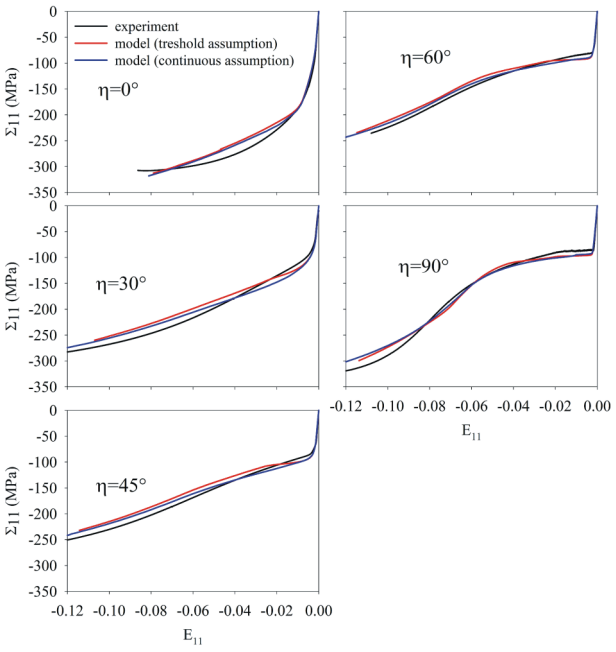

Fig. 2. Obtained stress-strain curves compared with model predictions. The compression load was performed for cylinders shown in Fig. 1.

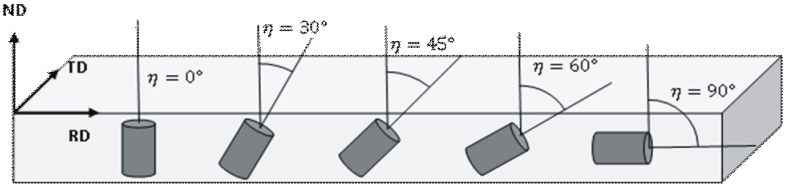

Fig. 1 Sample orientations selected for tests performed in different directions. The loading along cylinder axes were performed.

1. V. Hauk, *Structural and Residual Stress Analysis by Nondestructive Methods,* Amsterdam: ELSEVIER. 1997.

2. P. Kot, M. Wroński, A. Baczmański b, A. Ludwik, S. Wroński, K. Wierzbanowski, Ch. Scheffzük, J. Pilch, G. Farkas, *Measurement*, **221**, (2023), 113469.

This work was financed by a grant from the National Science Centre, Poland (NCN), No. UMO-2021/41/N/ST5/00394.

The research project was partly supported by the program "Excellence initiative – research university" for the AGH University of Science and Technology.

P. K. has been partly supported by European Union Horizon 2020 research and innovation program under Grant Agreement No. 857470 and the European Regional Development Fund via the Foundation for Polish Science International Research Agenda PLUS program Grant No. MAB PLUS/2018/8.

Measurements partly were carried out at the CANAM infrastructure of the NPI CAS Řež. The employment of the CICRR infrastructure supported by MEYS project LM2023057 is acknowledged.